ISSN (Print) : 0974-6846
ISSN (Online) : 0974-5645
Indian Journal of Science and Technology, *Vol 11(3), DOI: 10.17485/ijst/2018/v11i3/92398, January 2018*

Performance Comparison of Nature-inspired Optimization Algorithms Applied to MVDR Technique for Canceling Multiple Access Interference Signals

Suhail Najm Shahab*, Ayib Rosdi Zainun, Nurul Hazlina Noordin and Izzeldin Ibrahim

Faculty of Electrical and Electronics Engineering, University Malaysia Pahang, 26600, Pahang, Malaysia; 68suhel@gmail.com, ayib@ump.edu.my, hazlina@ump.edu.my, izzeldin@ump.edu.my

Abstract

Background/Objectives: Minimum Variance Distortionless Response (MVDR) beam forming technique is among the most widely used in antenna array field. The conventional MVDR has poor performance, and low Signal to Interference plus Noise Ratio (SINR) gain in the condition of limited snapshots or Multiple Access Interference (MAI) signals existing. Heuristic optimization algorithms are broadly used to solve many engineering problems. **Methods/Analysis**: In this work, two nature-inspired optimization methods, namely Particle Swarm Optimization (PSO) and Gravitational Search Algorithm (GSA) are applied to enhancing the conventional MVDR performance. In particular, the complex weight coefficients of the conventional MVDR solution are improved using both approaches. First, SINR calculated from MVDR basing linear antenna array configuration then the PSO and GSA implemented to minimizes the power of noise and interference in the constraint condition. The performance of the proposed methods is assessed based on various QoS criteria such as beampattern accuracy for azimuth and elevation scanning angles and SINR output. **Findings**: In comparison to conventional MVDR, the proposed algorithms have indicated that $MVDR_{GSA}$ providesfavorable agreement of synthesizing a maximum gain toward the desired real user angle while introducing deep null-forming in the undesired user directions. As a result, average SINR is evaluated over 20 runs in all simulation scenarios, the performance of $MVDR_{GSA}$ is better than the performance of $MVDR_{PSO}$. Moreover, a good control over the null-forming level can be achieved by $MVDR_{GSA}$ for iteration number < 100 whereas $MVDR_{PSO}$ is simple and easy to implement but required more convergence time to get high SINR. **Application/Improvements**: In general, it was observed that $MVDR_{GSA}$ out performs the $MVDR_{PSO}$ with respect to solution quality, stability and convergence speed.

Keywords: Beam Forming, Linear Antenna Array, Smart Antenna, GSA, MVDR, PSO, SINR

1. Introduction

Wireless communication systems and especially the cellular sector are among the leading technologies that have made a significant impact on society. Wireless communication systems have been gaining more popularity due to their added versatility and flexibility. Radio frequency interference continues to be a persistent problem in many communication systems and will potentially exacerbate as the unused wireless spectrum continues to shrink. There are, in general, two types of interfering signals; a) Intentional jammers used in military applications, such

*Author for correspondence

as electronic warfare (EW). b) Unintentional, yet harmful interference, primarily associated with commercial wireless systems[1]. Smart Antenna Systems (SASs) provide a promised solution for wireless network due to the ability to reduce the effects of Multiple Access Interference (MAI) signals.

The ABF methods have gained wide attention by researcher's community due to the wider range of application. Minimum Variance Distortionless Response (MVDR) or Capon beam former[2] is one of the adaptive optimum statistical beam formers which assures a distortion less response for a predefined steering direction[1,3,4]. The basic idea of the MVDR technique is to estimate the beam forming excitation coefficients in an adaptive manner by minimizing the variance of the residual interference and noise while enforcing a set of linear constraints to ensure that the real user signal is not distorted[5]. MVDR weight vector solution depends on the array response vector and the estimation of the covariance matrix of user-of-interest (UOI) signals and user-not-of-interest (UNOI) sources. The null-forming for MVDR has poor SINR output due to low null-forming level towards the UNOI signals when multiple access interference isexisting[6-9], the finite size of data snapshots[10,11] or the array response vector uncertainty[12,13].

There are many ways to make the MVDR beam former robust against this error such as diagonal loading[14] or beam space processing[15]. This empirical framework does not always lead to a solution that is easily identifiable, and therefore, optimization can be applied to provide a more robust solution which provides optimal performance for the SAS. Some researchers have presented numerical techniques involving nature-inspired optimization to improve the antenna beampattern, beam width and side lobe control, phase shifter, or complex weight vector of conventional beam forming techniques[6,8,16-20]. A study in[8] combines the Linear Constrain Minimum Variance (LCMV) beam former technique introduced[21] with Particle Swarm Optimization (PSO), Dynamic Mutated Artificial Immune System (DM-AIS), and GSA to improve and optimize the complex excitation coefficients of LCMV beam forming technique. The most effective solution founded by GSA algorithm among other for all simulation results. Similarly, [22] proposed a phase-only pattern optimization by using GSA based on concentric ring antenna array of reconfigurable dual-beam. In [23] compares the MVDR and delay and sum (DAS) beam former by using different matrix inverse method. The finding proved that the MVDR outperforms DAS through FPGA implementation with narrow mainlobe beam width and lower side lobe level. Some studies are done to combine GSA with Direction of Arrival (DoA) method based adaptive antenna array system for enhancing the accuracy of DoA estimation of the incident angles[24]. Applied GSA and modified PSO to reduce the side lobe effects in the antenna beampattern. Among these studies, GSA gives a superior performance or at least comparable improvement than others. In[6] the authors combined two intelligent swarm algorithms to improve the MVDR weight vector. Unfortunately, it does not clearly stated the noise power of the received signals, because the noise power has a significant impact on the MVDR null-forming[25,26]. On the other hand, the effects of population size and a number of maximum iteration also not explicitly mentioned and investigated. Thus, the solution of this study is not the most accurate one.

In this study, the null-forming of the MVDR technique is improved using two intelligent swarm algorithms namely, PSO and GSA. The performance evaluation for the comparison purpose is based on two figure of merit, SINR and beampattern accuracy which is still unknown from the expressions. The null width in the azimuth and

elevation scanning angle also have been assessed. The weights excitation coefficients calculated to place deep and sharp nulls toward the UNOI direction accurately and unity gain response toward the direction of UOI. Simulation results confirm the accuracy of the numerical results. The outline of this work is organized as follows: section 2, proposed two ABF methods along with the conventional MVDR system model is described. Section 3, highlight the significant outcomes from MVDR based PSO these combinations. Lastly, the conclusion is given in the last section.

2. MVDR Beam Former Design Model

The basic theory of the beam forming algorithm and the signal structure is presented in this section. The signal model considers L sources incident on a Uniform Linear Array (ULA) of M isotropic antenna elements, and the spacing between neighboring antennas is a half of wavelength. Assume that L signal coming from angles of θ_l and ϕ_l is incident upon an antenna array of M elements as shown in Figure 1. Here, the impinging angles of θ and ϕ are the azimuthally and elevation angles, respectively.

The received signal, $r_m(k) \in \mathbb{C}^{M\times K}$, at them th antenna at the k^{th} snapshot incident upon the antenna array can be written as:

$$r_m(k) = \sum_{s=1}^{S} x_s(k)\hat{a}_s(\theta,\phi) + \sum_{i=1}^{I} x_i(k)\hat{a}\,(\theta,\phi) + \sum_{m=0}^{M} n_m(k) \tag{1}$$

where, $x_s\,(k)$, $x_i(k)$, and $n_m(k)$ denote the s^{th} user-of-interest (UOI) signals, I^{th} interference signals and additive

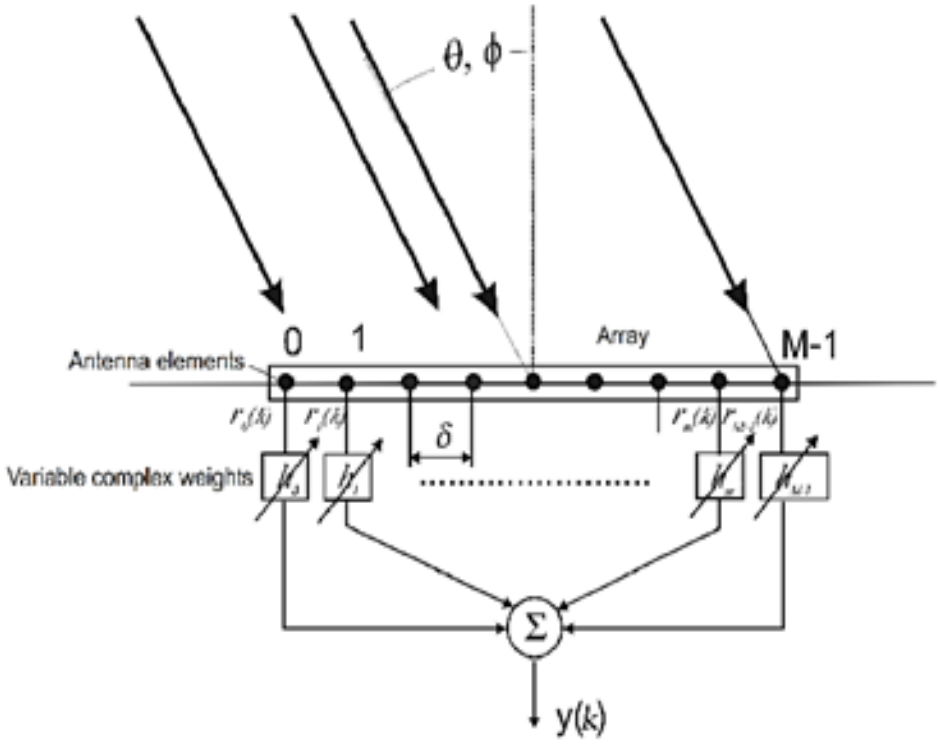

Figure 1. Uniform Linear antenna array geometry.

background White Gaussian noise at them th elements, respectively. Among those L incident signals, it is assumed that $x_s(k)$ is the desired UOI and $x_i(k)+n_m(k)$ are the user-not-of-interest (UNOI) signals. The array response vector, $\hat{a}(\theta_l,\phi_l)$ is a $\in\mathbb{C}^{M\times l}$ of a ULA with M-elements where (θ_l,ϕ_l) are the DOAs of the l^{th} signal component give as[4,27]:

$$\hat{a}(\theta,\phi)=[1,e^{-j\beta\delta\sin\theta\sin\phi},\ldots,e^{-j(M-1)\beta\delta\sin\theta\sin\phi}]^{*} \quad (2)$$

where, $\beta=2\pi/\lambda$ is the free-space wave number, δ is the separation between two elements and λ is the free-space wavelength. The $\theta\in[-\pi/2, \pi/2]$,$\phi\in[0, \pi/2]$ and $(.)^{*}$denote the complex conjugate. The $\hat{a}(\theta_l,\phi_l)$ is a function of the incident angles, the location of the antenna, and the array geometry. It plays an important role in smart antenna systems, containing information of the impinging angles. The output of the beam former at the k^{th} snapshots, y(k) after signal processing is defined as:

$$y(k)=\sum_{m=1}^{M}h_m^{\dagger}r_m(k) \quad (3)$$

where, h is a complex multiplicative weight vector given as $[h_0,h_1, \ldots ,h_m,h_{M-1}]^{T}$ multiplied by the received signal at the m^{th} antenna element and $(.)^{\dagger}$, $(.)^{T}$ denotes respectively the complex conjugate transpose of a vector or matrix and transpose of a vector or matrix. The array cross-correlation (covariance) matrix $\mathbf{\Gamma}_r\in\mathbb{C}^{M\times M}$ matrix, is defined as[28]:

$$\tilde{\mathbf{A}}_r=\{r_m(k)\times r_m^{\dagger}(k)\} \quad (4)$$

The array covariance matrix $\mathbf{\Gamma}_r$ in Equation (4) is the second-order statistical property of the impinging signals. In real applications, $\mathbf{\Gamma}_r$ is estimated using the received array snapshots. The estimated array covariance matrix is given by[3]:

$$\tilde{\tilde{\mathbf{A}}}_r\cong\tilde{\mathbf{A}}_d+\tilde{\mathbf{A}}_{i+n}\cong\frac{1}{K}\sum_{k=1}^{K}r_m(k)r_m^{\dagger}(k) \quad (5)$$

$$\tilde{\mathbf{A}}_s=\sum_{s=1}^{S}\sigma_s^2\hat{a}_s(\theta,\phi)\hat{a}_s^{\dagger}(\theta,\phi) \quad (6)$$

$$\tilde{\mathbf{A}}_{i+n}=\sum_{i=1}^{I}\sigma_i^2\,\hat{a}_i(\theta,\phi)\,\hat{a}_i^{\dagger}(\theta,\phi)+\sigma_n^2\,\Lambda_m \quad (7)$$

where, K is the number of available snapshots. $\mathbf{\Gamma}_s$denotes the array correlation matrix corresponding to the desired UOI and $\mathbf{\Gamma}_{i+n}$ refer to the array correlation matrix corresponding to the undesired UNOI. The terms σ_s^2,σ_i^2 andσ_n^2 denotes the real user, interference, and noise powers. $\Lambda_m\in R^{M\times M}$ stands for the identity matrix. It is known from the literature that the optimization criterion for MVDR[2] forms weights in a way that will attempt to maintain unity gain of the beam former in the beam angle direction while steering nulls in the direction of interference[29]. The weights are calculated by solving the following minimization equations with unity gain restraint:

$$h_{MVDR}=\arg\min_{0\le h\le 1}\mathrm{E}\{|\mathrm{y(k)}|^2\} \quad (8)$$

$$\min_h h^{\dagger}\tilde{\tilde{\mathbf{A}}}_r h \;\; s.t. \;\; h^{\dagger}\hat{a}_s(\theta,\phi)=1 \quad (9)$$

The above equations are solved by using Lagrange multipliers, and the MVDR weight (h_{MVDR}) is given as[30]:

$$h_{MVDR}=\hat{a}(\theta,\phi)\,\tilde{\tilde{\mathbf{A}}}_r^{-1}[\hat{a}^{\dagger}(\theta,\phi)\,\tilde{\tilde{\mathbf{A}}}_r^{-1}\,\hat{a}(\theta,\phi)]^{-1} \quad (10)$$

Antenna radiation patterns are typically expressedin terms of radiated power. The output power is defined as[4]:

$$P_y = E\{y(k)y^{\dagger}(k)\} = h^{\dagger}E\{y(k)y(k)\}h = h^{\dagger}\tilde{\mathbf{A}}_r h \tag{11}$$

Equation (11) can be rewritten as:

$$P_y = h^{\dagger}\tilde{\mathbf{A}}_s h + h^{\dagger}\tilde{\mathbf{A}}_{i+n} h = P_s + P_{i+n} \tag{12}$$

$$P_s = \sum_{s=1}^{S} \sigma_s^2 \left| h^{\dagger}\, \hat{a}_s(\theta,\phi) \right| \tag{13}$$

$$P_{i+n} = \sum_{i=1}^{I} \sigma_i^2 \left| h^{\dagger}\, \hat{a}_i(\theta,\phi) \right| + \sigma_n^2 \tag{14}$$

where, P_s denote the power of the desired signal and P_{i+n} refer to the power output in the direction of UNOI. Finally, the SINR is defined as the ratio of the average power of the desired signal divided by the averagepower of the undesired signalcomputed as[31,32]:

$$SINR = \frac{P_s}{P_{i+n}} = \frac{\sum_{s=1}^{S} \sigma_s^2 \left| h^{\dagger}\, \hat{a}_s(\theta,\varphi) \right|}{\sum_{i=1}^{I} \sigma_i^2 \left| h^{\dagger}\, \hat{a}_i(\theta,\varphi) \right| + \sigma_n^2} \tag{15}$$

2.1 Particle Swarm Optimization (PSO)

While many nature-inspired optimization techniques have been proposed to the scientific community, most of these algorithms rely on the use of complicated operators (or mechanisms) which mimic naturally occurring processes. However, the Particle Swarm Optimization (PSO) technique uses very simple operators inspired by the birds flock formation founded[33,34]. Each particle in the swarm has an associated velocity, location in the coordinate solution system, personalbest-visited location (p_{best}), and global best-visited location (g_{best}) in the swarm has two memories: a cognizant memory and a social memory which are affiliated with the p_{best} and the g_{best} vectors, respectively. Naturally, each particle would like to revisit the area near its previously best-seen point. However, the particle is also aware of the best-seen point of the swarm and is torn between the two locations. Then, the velocity and the position of each particle in the swarm updated as:

$$v_i^d(t+1) = w(t) \times v_i(t) + c_1 r_1 (p_{best}^d(t) - x_i^d(t)) + c_2 r_2 (g_{best}^d(t) - x_i^d(t)) \tag{16}$$

$$x_i^d(t+1) = x_i^d(t) + v_i^d(t+1) \tag{17}$$

where, v_i^d(t) and x_i^d (t) denote the velocity and the position of i^{th} particle in the d^{th}dimension at the t^{th}generation,w is the inertia weight that decreases linearly, learning constants c_1 and c_2 values, r_1 and $r_2$random values in the interval of [0, 1][d].

2.2 Gravitational Search Algorithm (GSA)

Metaheuristic approaches have drawn considerable attention from many researchers in the last decade. One of the most popular metaheuristics are Gravitational Search Algorithm (GSA), GSA recently proposed colleagues[35] based on heuristic optimization inspired Newton's laws of motion and gravity. Newton's laws of motion, the second law of acceleration based on Newton's law of universal gravitation "Force acts on each agent to other agents in the universe. This force is directly proportional to the mass of the agents and inversely proportional to the square of the distance between the agents". In this section, it will introduce optimization algorithm based on the laws of gravity. This algorithm considered as mass measured individual objects and performances. All the force of gravity pulls objects with each other, and that causes a global move-

ment towards the heavier mass object. Therefore, they use the direct form of communication objects through gravitational forces. According to the best solution with heavier masses, which move more slowly than the lighter that guarantees the step of using this algorithm to find a better solution. Each agent in GSA has four specifications: position, inertial mass, active gravitational mass and passive gravitational mass. The position of the mass is suitable for solving the problem, and it isgravitational, and inertial masses decide to use an appropriate function. This mass will show an optimal solution in the search space.

In order to optimize such a problem, it is necessary to determine the search space. These solutions are defined in a particular search space to generate the initial i^{th} position of the N number of the individual agent randomly in the search space. Every possible solution is a mass for the GSA. The system is designed in this section will consist of several masses. The position of the masses as below:

$$x_i = (x_i^1, \ldots, x_i^d, \ldots, x_i^n); \; i = 1, 2, \ldots, N \tag{18}$$

where, x_i^d denote the position of the individual masses at the i^{th} agent in the d^{th} dimension of N-space dimension. At each generation, the best and worst of the calculated fitness value is selected for all agents and the improvements are made to maximize the problem defined as:

$$best(t) = \max_{j \in \{1,\ldots,N\}} fit_j(t) \tag{19}$$

$$worst(t) = \min_{j \in \{1,\ldots,N\}} fit_j(t) \tag{20}$$

where, *best* (t) and *worst* (t) is expressing the best and worst solutions in the iteration t, $fit_j(t)$ shows the fitness value and the suitability of individual jatmoment. Each mass is calculated with the current fitness value of the fitness function. The gravitational constant G, will be reduced exponentially in every generation, and is initially set to control the search accuracy. In other words, G is the function of the initial value (G_0) and t, computed as follows:

$$G(t) = G_0 \times e^{-\alpha \frac{t}{t_{\max}}} \tag{21}$$

where, G_0 is the initial value of the gravitational constant, a fixed value that the user determines, and t_{max} is the total number of iterations generations. The active mass in a gravitational mass of a search space based on passive gravitational mass and inertial mass by taking all masses equal to each other, the updated weight is calculated when evaluating the fitness through the following equation:

$M_{ai}=M_{pi}=M_{ii}=M_i$; i=1, 2… N

$$M_i(t) = \frac{m_i(t)}{\sum_{j=1}^{N} m_j(t)} \tag{22}$$

$$m_i(t) = \frac{fit_i(t) - worst(t)}{best(t) - worst(t)} \tag{23}$$

where, M_{ai}, M_{pi}, M_{ii}, M_i denotes respectively, the active gravitational mass of bodies, passive gravitational mass, inertia mass and i^{th} individual inertial mass. In Equation above normalization process is carried out, the heavy mass as determined by the mass update is the most effective. It moves slower than others that are more effective mass in the search space and attracts others better[22]. Then, by the laws of motion, the acceleration, $a_i^d(t)$, of the individual i at t^{th} generation in d^{th} dimension can be computed as:

$$a_i^d(t) = \frac{F_i^d(t)}{M_{ii}(t)} \tag{24}$$

where, $F_i^d(t)$ is the total force acting on a massis calculated after calculating the force between two masses:

$$F_i^d(t) = \sum_{\substack{j=1 \\ j \neq i}}^{N} rand_j F_{ij}^d(t) \quad (25)$$

where, $rand_j$ it is a random number in the range $[0, 1]^d$, and $F_{ij}^d(t)$ is the forces between two bodies that acting on the mass i fromjist defined as:

$$F_{ij}^d(t) = G(t)\frac{M_{pi}(t) \times M_{aj}(t)}{R_{ij}(t) + \varepsilon}(x_j^d(t) - x_i^d(t)) \quad (26)$$

where, M_{aj} associated with the j individual active gravitational mass, M_{pi} associated with the i individuals passive gravitational mass, $G(t)$ calculated at the same time, t, ε is a numerically small constant decided by a user. x_j^d(t), x_j^d(t) refer to i and jmasses and R_{ij} (t), the Euclidean distance between the two point masses in the search space (i and j members) it is calculated as:

$$R_{ij}(t) = \left\| x_i(t), x_j(t) \right\|_2 \quad (27)$$

All masses are accelerated in the search space interact with each other. Further, a next speed of the agent is considered part of the current speed state attached to its speed. Therefore, the new velocity and position at next iteration along the d^{th} dimension can be upgraded as follows:

$$v_i^d(t+1) = rand_i \times v_i^d(t) + a_i^d(t) \quad (28)$$

$$x_i^d(t+1) = x_i^d(t) + v_i^d(t+1) \quad (29)$$

where, $v_i^d(t)$ and $x_i^d(t)$ represents the velocity and the position of i^{th} agents at t^{th} iteration along with d^{th} dimension, respectively. By gravitational and inertial mass conformity assessment calculated in a simple manner. A heavier weight means more effective than an individual. It is better to have a greater attraction of the individual and is not meant slower moving it. The inertial mass and gravitational mass assuming equality values conformity of mass mapping are calculated.

The GSA algorithm is reminded of the need to use to prevent discovery initially remain in local optimum by checking *K best* of *N* agents to improve the discovery, and use will attract others. K best is the initial starting value and function decreasing with time in a certain way that includes the best fitness value, all individuals initially apply a force and is reduced with the passage of time and the resulting linear Kbest will only exert a force an individual to others. Therefore, Equation (25) can be changed as follows:

$$F_i^d(t) = \sum_{\substack{j \in Kbest \\ j \neq i}} rand_j F_{ij}^d(t) \quad (30)$$

The details on how to combine conventional theoretical MVDR with numerical techniques involving nature-inspired optimization is described in next section for using the weighted objective approach.

2.3 Problem Definition and Formulation

Null-forming methods are very important in modern communication systems for maximizing SINR. The most common MVDR problem is that the signal model must be quite accurate in order not to form unity gain in the UOI direction nulls in the direction of the UNOI. When the size of data snapshots is small will result in a poorly represented beampattern and degrades the MVDR performance. However, null-forming of the MVDR affected by these errors, therefore, the task of combine the conventional MVDR with nature-inspired metaheuristic

methods to find appropriate complex excitation coefficient that introducesdeep null-forming and hence high SINR can be obtained. Firstly, a population of agents is initialized with random position except the first set of agents replaced by the weight vector from MVDR $_{con}$ in the search space dimension and this position vector at specified dimension is converted to a candidate solution vector to this problem as shown in Equation 10. Afterward, the fitness function evaluated in each iteration to find SINR$|_{max}$ by minimizing power given to reach the UNOIs directions.

$$h_m^{\dagger} = x_N^d(t) = \begin{bmatrix} h_1 & h_2 & \cdots & h_M \\ x_1^1(t) & x_1^2(t) & \cdots & x_1^d(t) \\ \vdots & \vdots & \ddots & \vdots \\ x_N^1(t) & x_N^2(t) & \cdots & x_N^d(t) \end{bmatrix} \tag{31}$$

where, $\sum_{m=0}^{M-1} h_m^{\dagger} \in \mathbb{C}^{M\times 1}$is analogues to the x_N^d , where

N is the best solution for the total population size in each iteration with the number of variable in the search space dimension equal to the number of elements (M=d). In order to have a tradeoff between the antenna array and optimization method, the fitness function, ff can be calculated using the following equation

$$ff = \arg\max_{x_N^d} \left(\frac{P_s}{P_{i+n}}\right) s.t. \min P_{i+n} \tag{32}$$

where, P_s de note the power of the desired user and P_{i+n} refer to the interference and noise power. PSO and GSA are used to obtain the radiation pattern with SINR$|_{max}$. The goal of the apply optimization algorithm is to find complex excitation coefficients minimizing P_{i+n} provided that for a certain undesired angle resultant SINR$|_{max}$ values, on the other hand, desired user power satisfying the MVDR constrain of $x_N^d \widehat{a}_s(\theta,\phi) = 1$.

Termination criteria fixed by updating the algorithm until iteration reaches their maximum limit. Then return the best-so-far fitness value at the final iteration as the global fitness of the problem and the positions of the corresponding agent at specified dimensions as the global solution of that problem.

3. Simulation and Discussion Results

To simulate and investigate the effectiveness and accuracy of the both proposed models for placing minimum null-forming are discussed, where Mat lab® platform has been used to model the performance results regarding mathematical functions. In this study, a uniform linear array of 4, 8-antenna elements with0.5λ inter element spacing are used. Simulations were carried out for two different cases of one UOI and two UNOIs, and the best results are recorded after 20 simulated cycles. The standard PSO technique was applied to the SINR$|_{max}$ optimization problem with no further modifications to the algorithm described in section 2.1. The simulation parameters setting for the PSO algorithm used in the MVDR problem are shown in Table 1. The GSA algorithm discussed in section 2.2 was also applied to this problem for comparative purposes, and its parameters used for this problemare displayed in Table 1. MVDR based PSO (MVDR$_{PSO}$), MVDR based GSA (MVDR$_{GSA}$) are used to optimize adaptively the excitation weight coefficients of the array antenna system. The boundary conditions and the constraints are kept the same and are listed in Table 1.

Table 1. Key intrinsic parameters for MVDR, PSO and GSA

Key system parameters	Values
Array antenna configuration	ULA
Antenna type	Isotropic
Carrier frequency (*fc*)	2.6 GHz[14]
Beam scanning range [θ,ϕ]	[-90°:90°, 0°:90°]
Number of elements (*M*)	4, 8
Element spacing (δ)	$\lambda/2$
Snapshots (*K*)	250
SNR [dB] INR[dB]	10 10
UOI direction [θ_s°, ϕ_s°]	0,0
UNOI direction [θ_i°,ϕ_i°]	20,0 – 60,0
SINR target [dB]	Max
Population size (*N*)	10
Dimension of the search space (*d*)	4,8
Termination condition (t_{max})	100
Gravitational constant initial value (G_0)	100[35]
Gradient constant (α)	20[35]
Zero offset constant (ε)	2.22e-16[35]
self-learning coefficients (c_1=c_2)	2[33]
Random interval	*rand*[0, 1]^d
Time-varying inertia weight (w_{min}–w_{max})	0.4 – 0.9[33]
Fitness Limit	Max
Null-forming	Max

In the beginning, a signal was received by the smart antenna array system from the environment, which consisted of the desired signal (x_s) and also an undesired signal (x_i+n_m). The total received signal power assumed to be SNR=INR of 10 dB. The weight vector of each element depended on the incident angle and array covariance matrix estimation. In both cases, assumed that the incident angle is θ_s=0° and two interference sources located at the angles of θ_i = 20° and 60° in azimuth while the elevation angles are fixed of$\phi_s=\phi_i$=0°. The weight vector is calculated through the MVDR $_{con}$ with respect to a known direction of the users. The weight vectors obtained from MVDR $_{con}$ is usually not ideal. Hence, MVDR $_{con}$ based intelligent swarm technique will enhance the complex weight vectors by using Equations 31, and 32 to generate complex weight vector based on the initial weight vectors from MVDR $_{con}$ achieving maximum SINR.

3.1 Case 1

The first case simulation divided into two scenarios, in the first scenario illustrative comparison between the performance of the proposed MVDR$_{PSO}$, MVDR $_{GSA}$ and the MVDR $_{con}$ for M=4 whereas the second scenario uses the same assumption for M=8.The convergenceresults in from MVDR$_{PSO}$ and MVDR $_{GSA}$ are shown in Figure 2(a) by the 100th iterations and 10 populations per iteration with search dimension of 4-variables. It can be seen that the MVDR$_{PSO}$ and MVDR$_{GSA}$ demonstrated high fitness value (SINR) compared to the MVDR $_{con}$. Both algorithms started with roughly the same fitness value, and both were able to bring the best-so-far fitness up to approximately 87.37 dB and 126.45 dB, respectively at the final iteration which is a considerable improvement over the initial MVDR weight.

The radiation power plot of normalized beampatternis shown in Figure 2(b). It is observedthat both the MVDR$_{PSO}$ and MVDR$_{GSA}$ places a perfect null at each interference sources direction and maintaining a unity response for the UOI direction. However, the MVDR$_{GSA}$ places the deepest null at the interference signals. Meanwhile, MVDR$_{PSO}$ introduces better null toward the interference source than the MVDR $_{con}$. Furthermore, the average null for both interference sources are found to be -42.73 dB, -87.36 dB and -154.78 dB for MVDR $_{con}$, MVDR$_{PSO}$ and MVDR$_{GSA}$, respectively giving a ≈104% and 196% null improvements over MVDR $_{con}$. The obtained best-so-far SINR of the received signal for MVDR $_{con}$, MVDR$_{PSO}$ and MVDR$_{GSA}$ are 42.32 dB, 87.37 dB and 126.45 dB, respectively, and the mean-so-far SINR for MVDR$_{PSO}$ and MVDR $_{GSA}$ is 76.35 dB and 123.71 dB. Therefore, MVDR$_{GSA}$ algorithm seems to optimize the *ff* faster than MVDR$_{PSO}$; it can imply that the MVDR $_{PSO}$ algorithm is converging slowly towards the maximum SINR. In addition, MVDR $_{PSO}$ with a small number of searching iterations limits the quest for the best solution, which has also limited enhancements of the null-forming.

Figures 2(c)-(h) show the 3D beampattern for azimuthally and elevation scan angles plots of the MVDR $_{con}$, MVDR$_{PSO}$ and MVDR$_{GSA}$, respectively. The power is measured in dB and the color bar is used for a sense of the relative scale of the power. The inner rectangle dashed black line represents the null width that encompasses the UNOIs target while the main lobe represents by 'Main lobe' in all figures. It can be easily seen by comparing these figures, the null width in the θ° and ϕ° obtained by MVDR$_{GSA}$ narrower than MVDR $_{con}$ and MVDR $_{PSO}$ in addition to sharp null-forming. It is observed that the MVDR$_{GSA}$ give very deepest null-forming with a null width of almost ≤3° compared to 10° and 6° by MVDR $_{con}$ and MVDR$_{PSO,}$ respectively. The MVDR $_{con}$ and MVDR$_{PSO}$ main beam accuracy are skewed by 9° and 7° from the target direction while MVDR$_{GSA}$ provides accurately

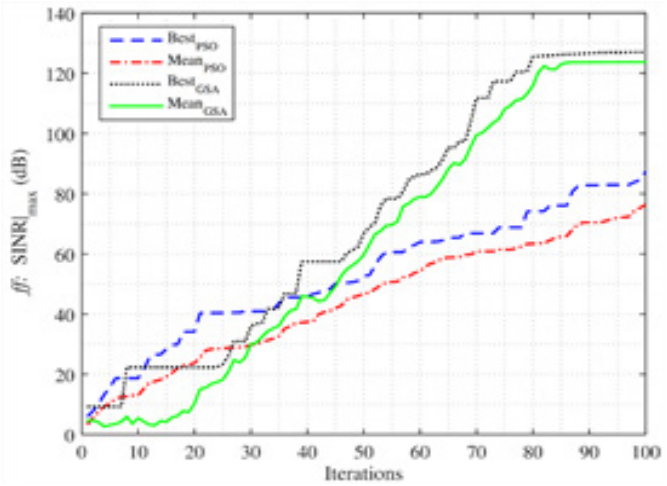
Best_PSO
Mean_PSO
Best_GSA
Mean_GSA
Iterations

(a)

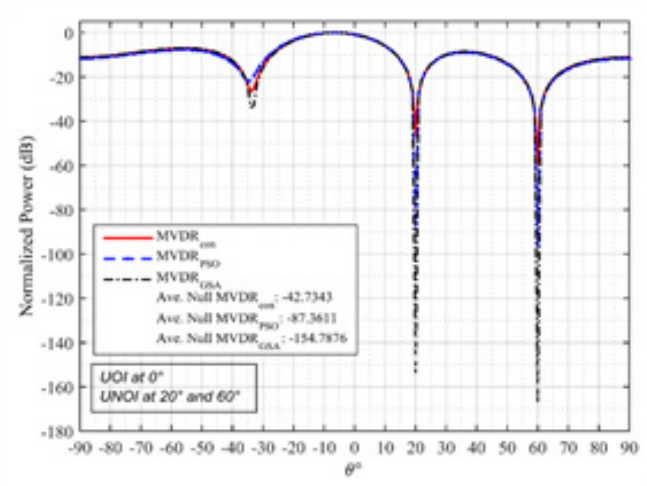
MVDR_con
MVDR_PSO
MVDR_GSA
Ave. Null MVDR_con: -42.7343
Ave. Null MVDR_PSO: -87.3611
Ave. Null MVDR_GSA: -154.7876
UOI at 0°
UNOI at 20° and 60°
Normalized Power (dB)

(b)

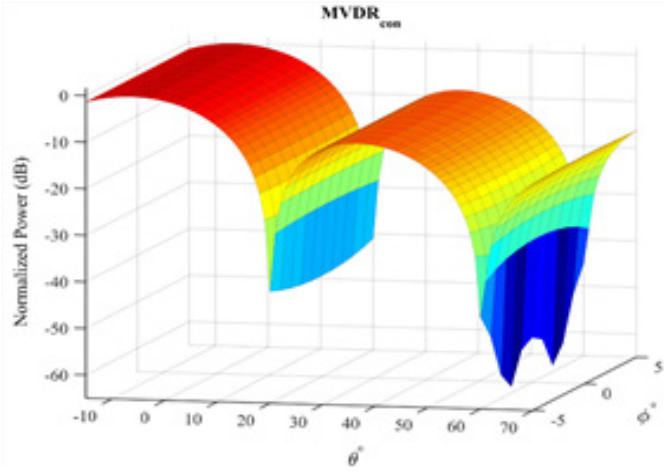
MVDR_con
Normalized Power (dB)

(c)

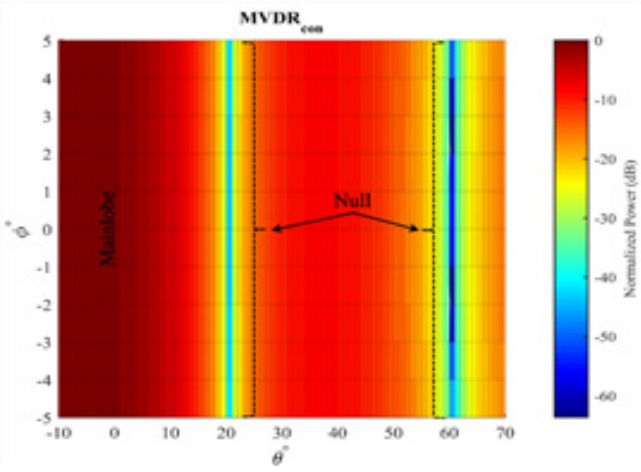
MVDR_con
Mainlobe
Null
Normalized Power (dB)

(d)

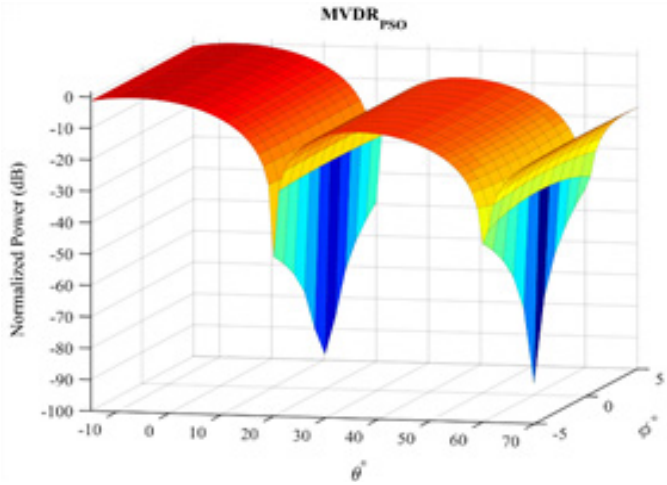
MVDR_PSO
Normalized Power (dB)

(e)

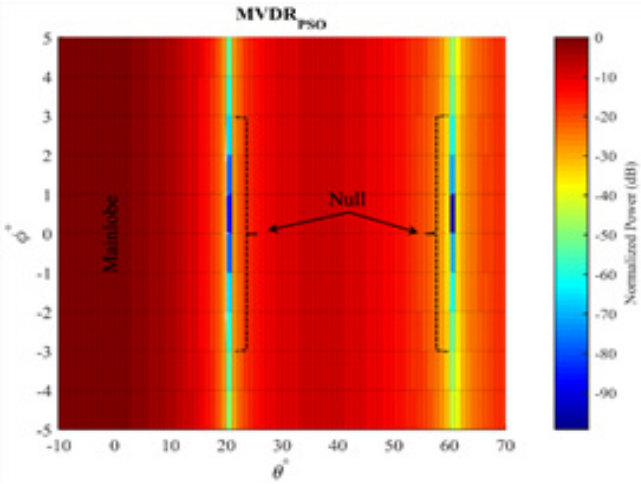
MVDR_PSO
Mainlobe
Null
Normalized Power (dB)

(f)

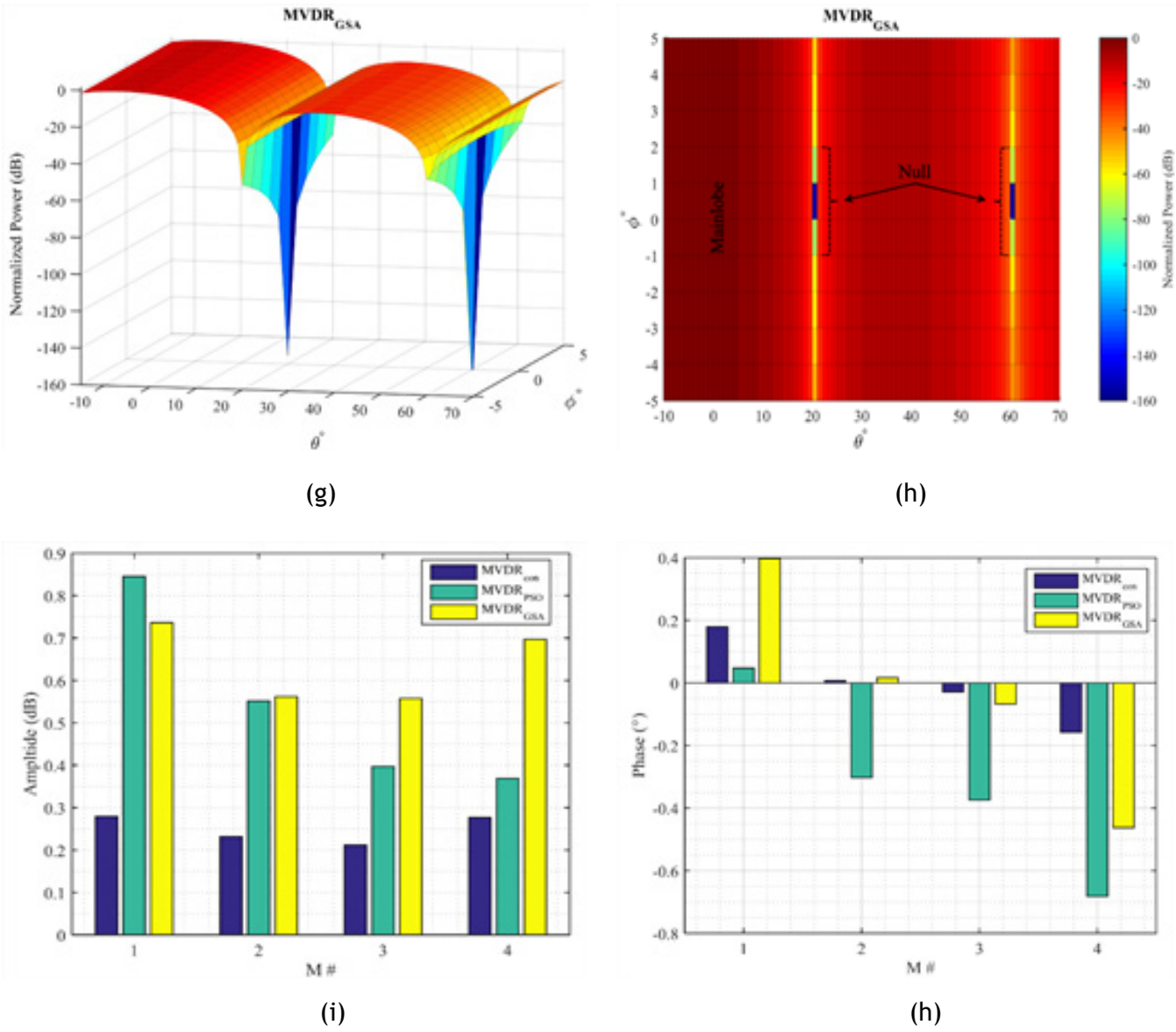

Figure 2. Comparison of SINR|max results between $MVDR_{con}$, $MVDR_{PSO}$ and $MVDR_{GSA}$; UOI at 0°, UNOIs at 20°, 60°, M=4, t_{max}=100, N=10; (a) Best and mean convergence rate. (b) Typical normalized beam pattern. (c)-(h) 3D beampattern in term of azimuth and elevation scan angles. (i)-(j) complex weights vector in term of amplitude and phase.

mainbeam of ≤1°. The corresponding best final solution (complex excitation weight) obtained from $MVDR_{con}$, $MVDR_{PSO}$ and $MVDR_{GSA}$ for each element are shown in Figure 2(i)-(j).

In the second scenario, the number of elements will be increased to 8and that is lead to the search space dimension also increased to 8-variavles with maximum iteration number set to 100th and population size set to

10. The results will be compared between the MVDR $_{con}$, $MVDR_{PSO}$ and $MVDR_{GSA}$. The two algorithms were applied to the optimization problem, and the convergence rate results are demonstrated in Figure 3(a). As expected, the best-so-far value for the $MVDR_{GSA}$ gave a good result effectively at a faster speed as compared to $MVDR_{PSO}$. In comparison, the improvement of SINR between $MVDR_{PSO}$ and $MVDR_{GSA}$ beam forming method for this scenario, the percentage of improvement would be 5% and 128%, respectively (from 46.99 dB, 49.19 dB and 107.17 dB). The mean SINR from $MVDR_{PSO}$ and MVDR $_{GSA}$ is found to be 35.8 dB, 105.9 dB, respectively.

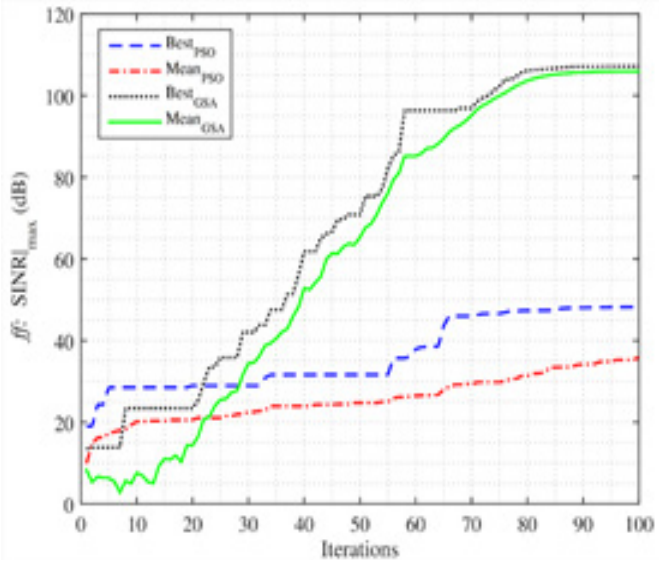

(a)

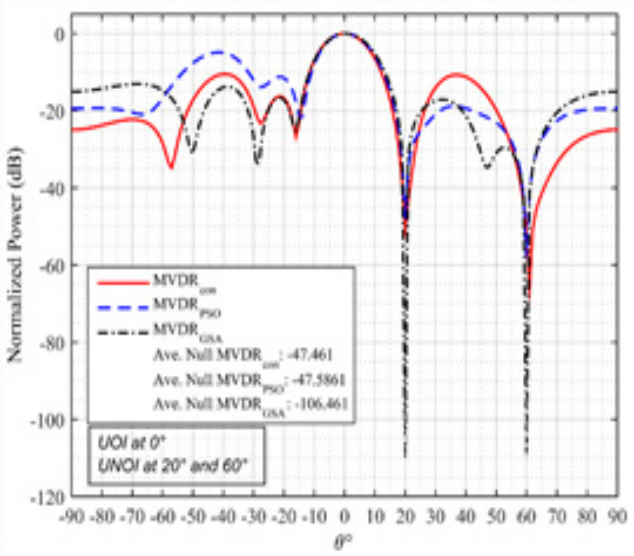

(b)

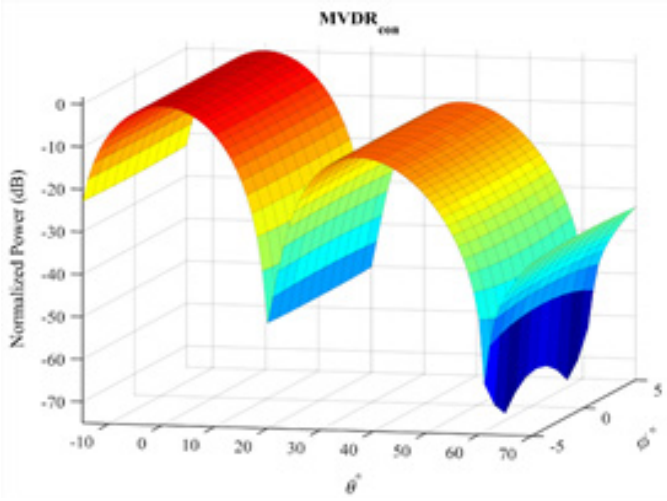

(c)

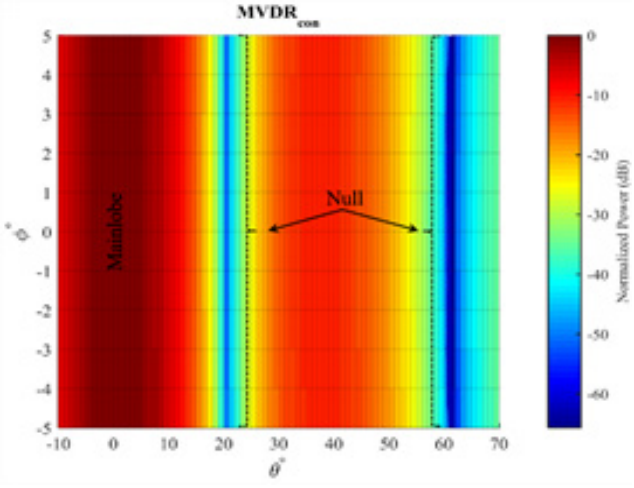

(d)

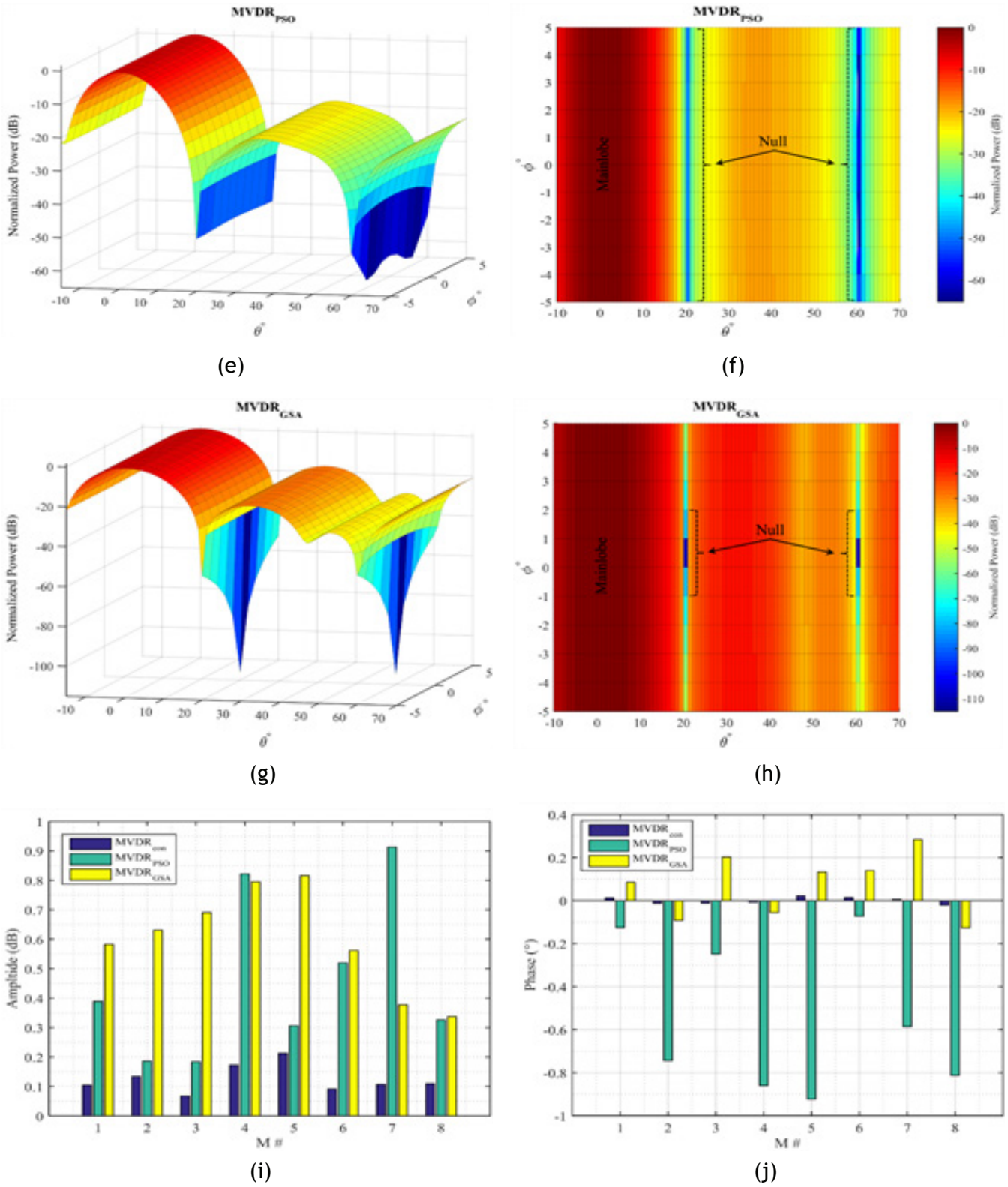

Figure 3. Comparison of SINR|max results between $MVDR_{con}$, $MVDR_{PSO}$ and $MVDR_{GSA}$; UOI at 0°, UNOIs at 20°, 60°, M=8, t_{max}=100, N=10; (a) Best ad mean convergence rate. (b) Typical normalized beam pattern. (c) - (h) 3D beampattern in term of azimuth and elevation angles. (i) - (j) Complex weights vector in term of amplitude and phase.

Figure 3(b) show the normalized rectangular radiation pattern, of the MVDR $_{con}$, $MVDR_{PSO}$ and $MVDR_{GSA}$ that nulls directed towards two co-channel interferences. It is clear from the radiation patterns in Figure 3(b), $MVDR_{GSA}$ model produces sophisticated solution that hasnegative average null powers below 106.46dBand this is regarded as the source of interference to the mainlobe, while the null-forming from $MVDR_{con}$ and $MVDR_{PSO}$ are found to -47.46 dB and -47.58 dB, respectively. Also, it can clearly be seen that the main lobe of the radiation patterns are directed toward the desired angles of UOI (θ_s=0°, ϕ_s=0°) in all the three methods. The null-forming improvements in percentage are about ≈ 1% and ≈ 124% for the $MVDR_{PSO}$ and $MVDR_{GSA}$, respectively, comparing to the MVDR $_{con}$. Hence, the $SINR|_{max}$ calculated from best weight vector for MVDR $_{con}$, $MVDR_{PSO}$, and $MVDR_{GSA}$ are found46.99 dB, 49.19dB and 107.17 dB. Moreover, the width of the main lobe decreases as the number of array elements is increased; in other words, it becomes narrower and high directivity.

The 3D beam pattern response for the MVDR con, MVDRPSO and MVDRGSA are shown in Figure 3(c)-(h), respectively. From the observation, the null width in the elevation angle is 10°, 10° and 3° for the $MVDR_{con}$, $MVDR_{PSO}$ and $MVDR_{GSA}$, respectively. In addition, the simulation result shows that $MVDR_{GSA}$ worked fine in exploring suitable excitation weight coefficients for optimized beam forming and subsequently obtained better SINR results. Besides, $MVDR_{GSA}$ worked fine in optimizing weight vectors through fixed number of iterations with increasing number of space dimension. It is evident MVDR $_{GSA}$ shows that lower nulling levels compared with $MVDR_{PSO}$ solution. However, for the 4-element array, there is a slight shift in the main beam placement by 1° by $MVDR_{GSA}$. Also, it is noted that the main beam width of the 8-element array is the narrowest while the 4-element array is the widest, with maximum side lobe level of -11.2 dB and -16.6dB, for $MVDR_{PSO}$ and $MVDR_{GSA}$ respectively. This is due to the directivity enhancement and the scanning resolution of the adaptive array antenna, which increases with the number of elements in the array. The required complex excitation of each element that resulting radiation pattern of $SINR|_{max}$ is shown in Figure 3(i)-(j).

<insert figure 3 here>

3.2 Case 2

A comparison between MVDR based PSO and GSA will be presented in this case; the results have been taken from 20-cycles and plotting the average of the $SINR|_{max}$ for a range of population size and iterations. Three population size have been considered to be N=10, 25, 50 each for the number of maximum iterations increased from 100th, 250thand 500th, in order to find the average solution resulted from both proposed methods. The user's direction and interference direction is similarly used from first simulation scenarios in case one. According to the results shown in Figure 4, the increases in the number of iterations has led to increases in the value of SINR owing to the increasing probability of finding better solutions within the search space. The main reason for adopting this process and the highlighting objective of using the deep and sharp null is to reduce the power distortions while increasing the SINR. For instance, at$N$=10 and t_{max}=100, the $MVDR_{PSO}$ slightly increased the SINR to 48.59 d B give ≈ 5% improvement compared to $MVDR_{GSA}$ of 118.47 dB (≈ 156% improvement), which is far better than the value obtained from MVDR $_{con}$ of 46.15 dB. On the other hand, at N=50 with the same t_{max}, the mean fitness for 20-cycle found to be 128.78 dB and 178.18 dB for $MVDR_{PSO}$ and $MVDR_{GSA}$ which give ≈ 179% and ≈ 286% improvements, respectively. By varying the number of iteration in each simulated cycle, the increases of t lead to give more chances to the exploration and exploitation of each algorithm to find higher SINR value at last iteration. Nevertheless, it is worthwhile noting that, any increases of iteration number for $MVDR_{PSO}$ after 250thcan only add

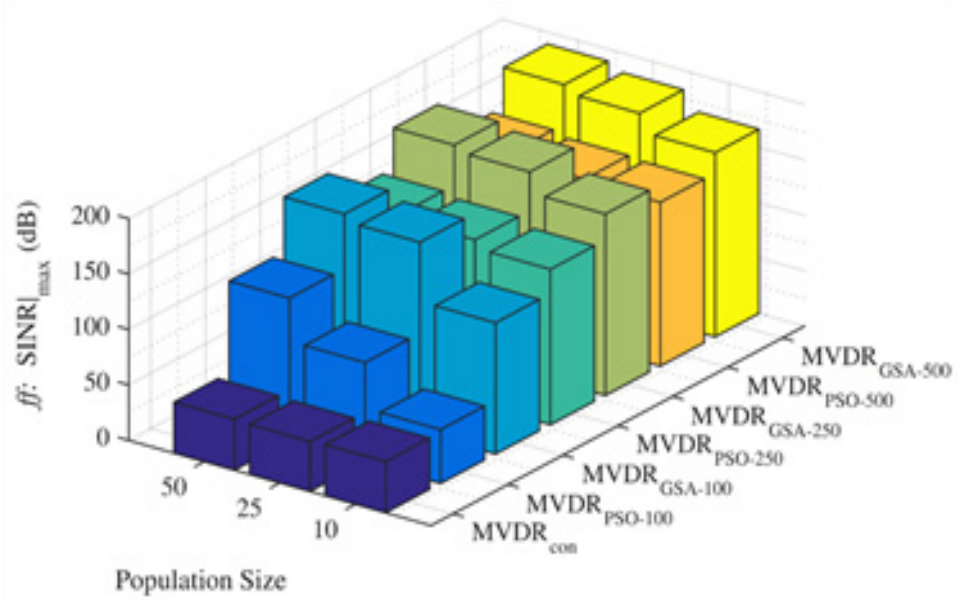

Figure 4. Performance comparison of average SINR for optimized $MVDR_{PSO}$ and $MVDR_{GSA}$.

a small SINR ratio improvement gradually. However, the correlation between MVDR and GSA is worth mentioning because of providing a significant SINR ratio for high iteration number and population size. The $MVDR_{GSA}$ technique proved to be the most effective algorithm according to the comparative analysis of both simulation scenarios in the previous section. The $MVDR_{GSA}$ technique was a better option as it offered a high convergence speed and its ability to get better fitness values within a short time frame. In terms of a solution and iterations, the $MVDR_{GSA}$ algorithm is faster and more accurate. The resultant SINR ratio on average for each technique has been demonstrated in Table 2 with its improvements value corresponding to $MVDR_{con}$.

As shown in Table 2, $MVDR_{GSA}$ results are clearly superior than $MVDR_{PSO}$ by using four elements of the antenna. It can be seenthat $MVDR_{con}$ has maximum SINR ratio in each trial with 46 dB at most. $MVDR_{PSO}$ has much SINR power enhancement around 153.54 dB while $MVDR_{GSA}$ has enormous SINR improvement of 189.14 dB. This is because the in crease in the dimensionality increases the number of points to be tested. With highly dimensional problems, the number of test points increases exponentially, therefore making the overall time required very lengthy. Notwithstanding, this improvement is because increasing N can point to increase the likelihood to find the complex excitation coefficient perfectly. This behavior is due to the fact that the GSA technique helps to explore the searching space with higher convergence rate, and thus it can produce a high-quality solution from the population of weight vectors because GSA search heuristics has its own set of search features that makes them capable of escaping local optima. Whilst PSO is known to have premature convergence rate issues.

Table 2. Average SINR ratio versus the effects of population size and the number of iterations

	N	$MVDR_{con}$	$MVDR_{PSO}$	$MVDR_{GSA}$	$MVDR_{PSO}$	$MVDR_{GSA}$	$MVDR_{PSO}$	$MVDR_{GSA}$
			t_{max} = 100		t_{max} = 250		t_{max} = 500	
$SINR\|_{max}$ (dB)	10	46.1519	48.5929 (5%)	118.4725 (156%)	140.2986 (203%)	163.7302 (254%)	147.8050 (220%)	166.1403 (259%)
	25	45.9034	89.7822 (94%)	171.8718 (272%)	147.6086 (219%)	179.7786 (289%)	149.6086 (224%)	182.5078 (295%)
	50	46.0409	128.7868 (179%)	178.1898 (286%)	151.2457 (227%)	187.5118 (306%)	153.5457 (232%)	189.1458 (309%)

To prove the importance and contribution of this findings, results of this work has been compared with previous LCMV[8] enhancement work for the smart antenna system. Therefore, the further comparison has been carried out to compare the results for MVDR and LCMV basing nature-inspired beam forming methods for average null level and maximum SINR output. Table 3 compares the average null-forming and output SINR. It can be seen that there is a noticeable difference between the $MVDR_{GSA}$ and $LCMV_{GSA}$ in term of the null-forming

Table 3. Performance comparison of beam forming techniques based optimization algorithms

Method	M	UOI	UNOIs	t_{max}	N	Ave. null (dB)	Max. SINR (dB)
$LCMV_{con}$ [8]	4	θ_s=0° ϕ_s=0°	$\theta_{i,1}$=20° $\phi_{i,1}$=0° $\theta_{i,2}$=60° $\phi_{i,2}$=0°	–	–	-1.1	4.4
$MVDR_{con}$				–		-42.7	42.3
$LCMV_{PSO}$ [8]				500	10	-50.5	56.1
$LCMV_{GSA}$ [8]						-84.0	80.6
$MVDR_{PSO}$				100		-87.3	87.3
$MVDR_{GSA}$						-154.7	126.4

level and output SINR, and this is due to LCMV required a more demanding computational load. Overall, $MVDR_{GSA}$ outperforms $LCMV_{GSA}$ in terms of output SINR by placing accurate and deep nulls in the direction of interferences. Therefore, the $MVDR_{GSA}$ seems to have stable performance.

4. Conclusion

Indeed, nature-inspired optimization techniques provide a unique tool that can find appropriate excitation coefficients solution where conventional beam forming algorithm often fail to provide deep nulls. They are still newly developed algorithms, and much more research has been going on to improve the various techniques. In this work, classical and modern heuristic optimization algorithms are used to enhance the MVDR performance. PSO and the GSA algorithms were introduced as possible candidates for using in array antenna system, and definitions were providedin every aspect of the SINR optimization formulation. Both algorithms were comparedin terms of convergence, efficiency, and robustness by the optimization of SINR mathematical fitness functions. The goal of this study is to provide minimal power to reach the UNOIs. Simulation results found nearly identical solutions which provided a minimal null in the MAI directions pecially by using GSA, the use of $MVDR_{GSA}$ method appears to be promising. Both PSO and GSA demonstrated good results for the null-forming optimization problems. However, the PSO algorithm had trouble with the maximization of the SINR for the iteration <100. As a conclusion, the combination of the MVDR and GSA beam forming algorithm has been decided to be a reasonable choice for the smart antenna application in the presence MAI sources.

5. Acknowledgement

This research was supported by University Malaysia Pahang, through the Fundamental Research Grant Scheme (FRGS) funded by Ministry of Education (RDU 140129).

6. References

1. Van THL. Optimum array processing: Part IV of detection, estimation, and modulation theory. 1st Edition. New York: Wiley; 2002.
2. Capon J. High-resolution frequency-wave number spectrum analysis. Proceedings of the IEEE. 1969; 57(8):1408–18. Crossref.
3. Gross F. Smart antennas with mat lab: principles and applications in wireless communication. 2nd Edition. McGraw-Hill Professional; 2015. p. 1–400.
4. Godara LC. Application of antenna arrays to mobile communications. II. Beam-forming and direction-of-arrival considerations. Proceedings of the IEEE. 1997; 85(8):1195-245. Crossref.
5. Pan C, Chen J, Benesty J. Performance study of the MVDR beam former as a function of the source incidence angle. IEEE/ACM Transactions on Audio, Speech, and Language Processing. 2014; 22(1):67–79.
6. Darzi S, Tiong SK, Islam MT, Ismail M, Kibria S. Optimal null steering of minimum variance distortion less response adaptive beam forming using particle swarm optimization and gravitational search algorithm. IEEE 2nd International Symposium on Telecommunication Technologies (ISTT). IEEE, Langkawi; 2014. p. 230–5.
7. Guney K, Durmus A. Pattern nulling of linear antenna arrays using backtracking search optimization algorithm. International Journal of Antennas and Propagation. 2015; 2015:1–10.
8. Darzi S, Sieh Kiong T, Tariqul Islam M, Ismail M, Kibria S, Salem B. Null steering of adaptive beam forming using linear constraint minimum variance assisted by particle swarm optimization, dynamic mutated artificial immune system, and gravitational search algorithm. The Scientific World Journal. 2014; 2014:1–10.

9. Mohammed JR, Sayidmarie KH. Null steering method by controlling two elements. IET Microwaves, Antennas and Propagation. 2014; 8(15): 1348–55. Crossref.
10. Ghadian M, Jabbarian-Jahromi M, Kahaei M. Recursive Sparsity-based MVDR Algorithm for Interference Cancellation in Sensor Arrays. IETE Journal of Research. 2015; 62(2): 1–9.
11. Chen YL, Lee JH. Finite data performance analysis of LCMV antenna array beam formers with and without signal blocking. Progress in Electromagnetic Research. 2012; 130:281–317. Crossref.
12. Wax M, Anu Y. Performance analysis of the minimum variance beam former in the presence of steering vector errors. IEEE Transactions on Signal Processing. 1996; 44(4):938–47. Crossref.
13. Besson O, Vincent FE. Performance analysis of beam formers using generalized loading of the covariance matrix in the presence of random steering vector errors. IEEE Transactions on Signal Processing. 2005; 53(2):452–9. Crossref. https://doi.org/10.1109/TSP.2004.840777
14. Malaysian communications and multimedia commission. SKMM-MCMC Annual Report [Internet]. 2011. Available from: http://www.skmm.gov.my/skmmgovmy/media/General/pdf/.
15. Feldman DD, Griffiths LJ. A projection approach for robust adaptive beam forming. IEEE Transactions on Signal Processing. 1994; 42(4): 867–76. Crossref.
16. Zaharis ZD, Yioultsis TV. A novel adaptive beam forming technique applied on linear antenna arrays using adaptive mutated Boolean PSO. Progress in Electromagnetic Research. 2011; 117:165–79. Crossref.
17. Liu F, Wang J, Sun C, Du R. Robust MVDR beam former for nulling level control via multi-parametric quadratic programming. Progress In Electromagnetic Research C. 2011; 20:239–54. Crossref.
18. Salem S, Kiong TS, Paw JKS, Hock GC. Artificial immune system assisted minimum variance distortion less response beam forming technique for adaptive antenna system. IEEE International Conference on ICT Convergence; 2013. p. 938–43.
19. Pavani T, Das RP, Jyothi AN, Murthy ASD. Investigations on Array Pattern Synthesis using Nature Inspired Met heuristic Algorithms. Indian Journal of Science and Technology. 2016; 9(2):1–11. Crossref.
20. Geethanjali V, Mohan T, Rao IS. Beamforming networks to feed array antennas. Indian Journal of Science and Technology. 2015; 8(S2):78–81. Crossref.
21. Widrow B, Mantey P, Griffiths L, Goode B. Adaptive antenna systems. Proceedings of the IEEE. 1967; 55(12): 1–17. https://doi.org/10.1109/PROC.1967.6092 Crossref.
22. Chatterjee A, Mahanti GK, Mahapatra PRS. Design of fully digital controlled reconfigurable dual-beam concentric ring array antenna using gravitational search algorithm. Progress in Electromagnetic Research C. 2011; 18:59–72. Crossref.
23. Hema N, Kidav JU, Lakshmi B. VLSI Architecture for Broadband MVDR Beamformer. Indian Journal of Science and Technology. 2015; 8(19):1–10. Crossref.
24. Magdy A, Mahmoud K, Abdel-Gawad S, Ibrahim I. Direction of arrival estimation based on maximum likelihood criteria using Gravitational Search Algorithm. PIERS Proceedings. Taipei. 2013; 28:1162–7.
25. Shahab SN, Zainun AR, Mohamed II, Noordin NH. The impact of noise label on beampattern and SINR of MVDR beamformer. International Journal of Computing, Communication and Instrumentation Engineering. 2016; 3(1):89–95.
26. Shahab SN, Zainun AR, Noordin NH, Mohamad AJ. Performance analysis of smart antenna based on MVDR beam former using rectangular antenna array. ARPN Journal of Engineering and Applied Sciences. 2015; 10(22):17132–8.
27. Godara LC. Smart antennas. Boca Raton: CRC Press; 2004. p. 1–458. Crossref.
28. Krim H, Viberg M. Two decades of array signal processing research: the parametric approach. IEEE Signal Processing Magazine. 1996; 13(4):67–94. Crossref.
29. Souden M, Benesty J, Affes S. A study of the LCMV and MVDR noise reduction filters. IEEE Transactions on Signal Processing. 2010; 58(9):4925–35. Crossref.
30. Balanis CA, Ioannides PI. Introduction to smart antennas. Arizona, USA: Morgan and Claypool Publishers. Synthesis Lectures on Antennas. 2007; 5:1–179. Crossref.
31. El Zooghby A. Smart antenna engineering. Norwood, MA, USA: Artech House, Inc; 2005. p. 1–10.

32. Dosaranian-Moghadam M. Joint adaptive beam forming and perfect power control in wireless networks over power control error. Indian Journal of Science and Technology. 2012; 5(10):3390–402.
33. Kennedy J, Eberhart R. Particle swarm optimization. Proceedings of IEEE International Conference on Neural Networks. Perth, Australia; 1995. p. 1–7. Crossref.
34. Eberhart RC, Kennedy J. A new optimizer using particle swarm theory. Proceedings of the Sixth International Symposium on Micro Machine and Human Science. New York, NY; 1995. p. 39–43. Crossref.
35. Rashedi E, Nezamabadi-Pour H, Saryazdi S. GSA: A gravitational search algorithm. Information Sciences. 2009; 179(13):2232–48. Crossref.